IIETA International Information and Engineering Technology Association
Advancing the World of Information and Engineering

Journal of New Materials for Electrochemical Systems
Vol. 27, No. 3, August 2024, pp 270-275
Journal homepage: http://iieta.org/journals/jnmes

Analyzing Metal Material Cooling Intensity: A Method for Obtaining Heat Transfer Coefficients

Deepa Melur Sonnegowda[1], Lalitha Ponsankarar[2], Vinay Kumar Domakonda[3], Kamesh Minnal Ranjan Babu[4], Vinayak Barewar[5], Vijay Muni Tadanki[6], E.Hemalatha [7], Anusuya Manickam[8], Aravind Prasad Baskaran[9*] and Selvarajan Lakshmanan[10]

[1] Department of Aeronautical Engineering, SJC Institute of Technology, Chikkaballapur, Karnataka 562101, India
[2] Department of Physics Indra Ganesan College of Engineering, Trichy, Tamil Nadu 620012, India
[3] School of Engineeringnd Computing, American International University, Kuwait
[4] Department of Mechanical Engineering, Dayananda Sagar College of Engineering, Bangalore 560111, India
[5] Department of Mechanical Engineering, Indira Gandhi Engineering College,Sagar, Madhya Pradesh 470021, India
[6] Department of Electrical and Electronics Engineering, Koneru Lakshmaiah Education Foundation, Vaddeswaram, Andhra Pradesh 522302, India
[7] Department of Physics, Karpagam College of Engineering (Autonomous), Coimbatore 641032,Tamilnadu, India
[8] Department of Physics, Indra Ganesan College of Engineering, Trichy, Tamil Nadu 620012, India
[9] Department of Artificial Intelligence, K. Ramakrishnan College of Technology, Tiruchirappalli 621 112, Tamilnadu, India.
[10] Department of Mechanical Engineering, Mahendra Institute of Technology (Autonomous), Namakkal District, Tamil Nadu, 637 503, India

*Corresponding Author Email:*aravindprasadpb.ai@krct.ac.in*

https://doi.org/10.14447/jnmes.v27i3.a12

Received: 28-02-2024
Accepted: 25-08-2024

Keywords:
Laminar cooling, heat transfer coefficient, temperature field, sine amplitude, sine period

ABSTRACT

In laminar cooling, the cooling intensity is directly impacted by the heat transfer coefficient and affects the microstructure of metal materials, which in turn affects product performance. In order to determine the laminar cooling heat transfer coefficient, this study suggests a certain approach. Using the nozzle as the center, the dispersal form of coefficient of heat transfer as piecewise function formed a straight line and half sine wave was determined. It lays out the steps to take in experimental data, operating parameters, and structural parameters to get function's characteristic parameters. Experimental results confirm the method's correctness, and the effect of metal-specific characteristics on the temperature field was studied. A solid theoretical foundation for the field production process was provided by the mutual verification of the experimental and computed outcomes.

1. INTRODUCTION

Humans will be subjected to increasing environmental pressure and resource scarcity as the metallurgical industry continues to advance and grow [1]. The significance of controlled cooling for medium and heavy plates is growing in this setting. Among the many critical variables in plastic deformation of metals, temperature ranks high. When it comes to hot rolling, controlling a single point temperature like the finishing or coiling temperatures is usually more important for achieving qualifying qualities and rolling stability. Few studies have examined the effects of transverse temperature fluctuation on strip steel's microstructure, mechanical and physical properties, and the likelihood of defects following laminar cooling [2]. In order to handle medium and heavy plates, the model relies on the comprehensive coefficient of heat transfer.

The new group of steel materials called low-carbon bainitic steel has emerged, built on the principles of microstructure control and theory of fine grain steel [3]. A limited quantity of martensite, thin-film preserved austenite, and ultra-fine nano bainite lath make up microstructure of low-carbon steel. It forms foundation of unique qualities exhibited by these steels. Important to the steel's quality is a heat treatment that happens at laminar cooling next to rolling; this achieves the correct ratio of ferrite to martensite volume percentage. However, it is not a picnic to get the coefficient of heat transfer correct in the process [4]. It is due to designing ideal cooling settings relies heavily on computational models of phase transitions that occur during cooling. The coefficient of heat transfer on surface of metal cannot be simply calculated due to the complexity of the laminar cooling heat transfer mechanism [5]. Currently, researchers primarily employ one of two approaches to derive this coefficient: mathematical measurement algorithms or empirical formula method.

Combining numerical simulation with the empirical formula technique is a common practice for forecasting the curl, field temperature of metal materials. The impact of nozzle spacing, water flow rate, nozzle diameter, and cooling water temperature on cooling capacity has been investigated by some researchers utilizing their proprietary software for performance prediction and microstructure based on metallurgical models. The empirical formula technique was employed in these studies [6], [7]. When metals undergo phase change latent heat during laminar cooling, a number of studies have shown that predicting their temperatures more accurately requires a combination of heat transfer and phase change models [8], [9]. The heat transfer coefficient can be calculated in two different ways. In order to begin, the various elements that influence cooling by performing experiments utilizing the

inverse heat transfer method were investigate [10]. The second method predicts density of heat flux in cooling zone of water for hot rolling layer utilizing a regression model that integrates past data and production statistics from the field. The resulting model is then used to predict the curl temperature [11]. In comparison to the multiple regression method, the BP neural network method outperforms it when it comes to predicting heat flux density. While there are cases were using an field data regression method or empirical formula makes meaningful, these methods have their limitations and are susceptible to errors caused by variations in production settings. But, it was finding the time-dependent distribution of the heat transfer coefficient using solution method for reverse heat transfer problems; however, this distribution is only useful under certain manufacturing circumstances. To find the rule of influence between coefficient of heat transfer and the field of temperature, large-scale tests were required.

The defining characteristics of the laminar cooling heat transfer coefficient function are derived from the aforementioned research using structural factors, operational parameters and data field. The effect of these defining features on temperature distribution of metallic materials was further investigated. In mathematics, characteristic parameters provide a way to describe the outcomes of controlling manufacturing operations. As a result of its relevance in directing production, a change in characteristic parameters represents a change in the operation control process.

2. METHODOLOGY

The placement of the nozzles in each row divides the laminar cooling area into multiple portions. Within injection region of every row of nozzle, coefficient of heat transfer follows a sinusoidal distribution, and between neighboring sinusoidal functions, it is nearly linear. The heat transfer coefficient with direction of cooling for the metal material is distributed by a piecewise function that is composed of a straight line and a sine curve.

As an example, Equation (1) shows the coefficient of heat transfer as a sine function, using the nth region [12], [13]:

$$h_{s,n} = A \cdot \sin\{\omega\{\tau - [(2n-3)\phi_c + (n-1)\phi_0]\}\}, \quad (1)$$

$h_{s,n}$ is coefficient of convective heat transfer in nth iteration. The sinusoidal function amplitude was denoted by s, is equal to the square root of the angular frequency, denoted as τ, divided by sinusoidal function period, and the time gap among adjoin sinusoidal functions is denoted as φ-0.

Equations (2) through (4) demonstrate the linear distribution of the heat transfer coefficient:

$$h_{a,n} 2.15\left(T_{\omega,\tau} + T_a\right)^{\frac{1}{4}}, \quad (2)$$

$$h_{\tau,n} = \sigma\varepsilon\left(T_{\omega,\tau} + T_a\right)\left(T_{\omega,\tau}^2 + T_a^2\right), \quad (3)$$

$$h_{1,n} = h_{a,n} + h_{\tau,n} \quad (4)$$

$$h_{s,n} = \begin{cases} A \cdot \sin\{\omega\{\tau - [(2n-3)\phi_c + (n-1)\phi_0]\}\} \\ 0 \le \tau < \phi_c \qquad (n=1) \\ [(n-1)\phi_0 + (2n-3)\phi_c] \le \tau < [(n-1)\phi_0 + (2n-1)\phi_c] \quad (n = 2,3,\dots,n-1) \\ [(n-1)\phi_0 + (2n-3)\phi_c] \le \tau \le \frac{L}{V} \qquad (n=n) \\ 2.15\left(T_{\omega,\tau} - T_a\right)^{\frac{1}{4}} + \sigma\varepsilon\left(T_{\omega,\tau} + T_a\right)\left(T_{\omega,\tau}^2 + T_a^2\right) \\ [(n-1)\phi_0 + (2n-1)\phi_c] \le \tau \le [n\phi_0 + (2n-1)\phi_c] \qquad (n = 1,2,\dots,n-1) \end{cases} \quad (5)$$

V represents the speed at which metal materials run in m/s, and L represents the length of the cooling section in meters.

The main focus of cooling metal materials is the sine-function distribution of heat transfer coefficients. Characteristics of the function distribution are reflected in the angular frequency (period), sine function's amplitude, and beginning phase. Laminar cooling is characterised by three variables: amplitude, angular frequency, and commencement phase, which represent the cooling strength, duration, and starting point of the nozzle relative to the water.

As seen in Equation (6): the sinusoidal function's angular frequency was determined by using both structural and operating factors [14].

$$\omega = \frac{2}{4(H_0 - H_b)\tan\beta} \quad (6)$$

β is the injection angle, H-o is the thickness of the metal substance in millimeters, and n-o is the height at which the nozzle is installed (rad). Fig 1 clearly shows that it is equal to one quarter of the sine function's duration. As demonstrated in formula (7) it can be determined using formula (6) [15], [16].

$$\phi_c = \frac{(H_o - H_b)\tan\beta}{V}. \quad (7)$$

The size of,φ-0. is influenced by both structural characteristics and operating parameters, as seen in Equation (8):

$$\phi_o = \frac{B - (H_o - H_b)\tan\beta}{V} = 2\left(\frac{B}{2V} - \phi_c\right), \quad (8)$$

in which B denotes the separation between the two nozzles.

Numerous parameters, including spray height, pressure, spray flow rate, and impact the amplitude M, making it impossible to directly provide the calculation relationship. Using experimental data and an optimization technique, one may determine the value of amplitude a. Equation (9) shows the objective function of the optimization process [17], [18]:

$$A = \min \sum_{i=1}^{n} (x_i - x_i')^2. \quad (9)$$

In the given equation, n represents the total number of authentic measurements, x-i. stands for the temperature (N) computed by ith time of heat transfer model and xi' denotes the temperature of ith detection time.

The field equipment is used as a study object to analyze the impact of parameter characteristic on temperature field, in accordance with proposed method for obtaining coefficient of heat transfer for laminar cooling.

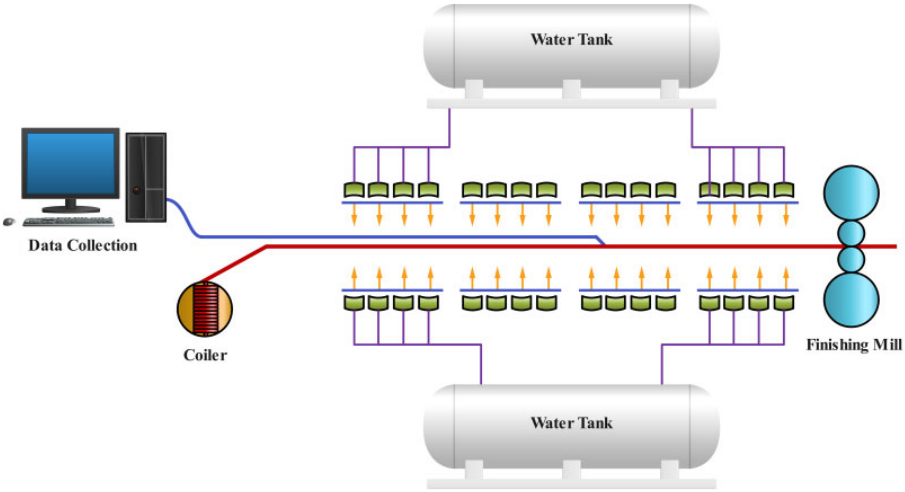

Figure 1. Production line test chart for laminar cooling

The metal material has a size of 20 m x 2.5 m x 30 mm, a running speed of 2.7 m/min, a vertical distance of 520 mm between the nozzle and the material, and a spacing of 280 mm between two nearby nozzles. Before filling the hole with refractory mud, the surface and middle temperatures of metal components were monitored. This is followed by welding the thermocouple at 1 to 14 mm from distance table to bottom hole. The three spots were choosed to monitor the surface temperature and two spots to measure the inside temperature. The model's predicted value is contrasted with the mean temperature. Fig 2 displays the heat transfer coefficient distribution after calculation, with an injection angle H of $\pi/12$. Fig 4 displays the coefficient of heat transfer distribution after calculation, with the injection angle β equal to $\pi/12$.

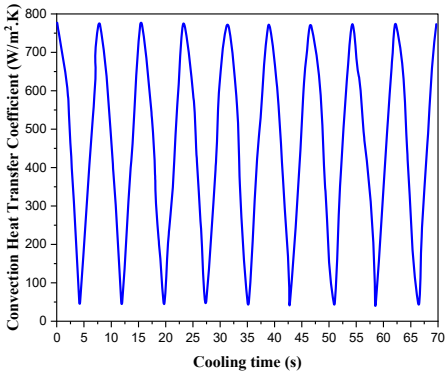

Figure 2. Laminar cooling's convective heat transfer coefficient

3. MODEL VALIDATION

The model's predictions of the metals' surface and central temperature distributions were compared with their experimental findings after plugging in the measured heat transfer coefficient. Fig 3 displays the outcomes. The metal material's temperature drops as it moves under the nozzle, as shown in the Fig 3 and it changes as it goes through nozzle meters each row. Surface temperature does not seem to be changing, though, because of the temperature variation at the base of the nozzle.

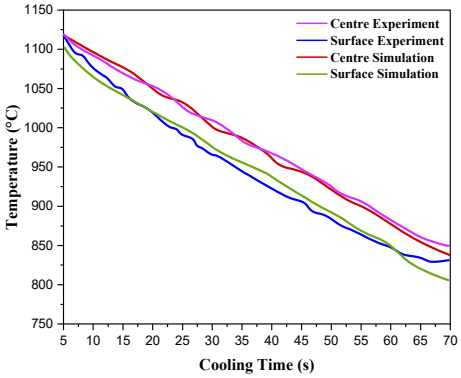

Figure 3. Comparison of the temperature determined by experiment and the temperature predicted by the model

4. RESULTS AND DISCUSSIONS

Heat transfer coefficients are defined by their amplitude, period, and beginning phase, among other factors. While period and beginning phase are connected parameters, amplitude was the independent variable of the temperature field. This is mostly due to the fact that structural features in laminar cooling impose limitations on the boundary shape of heat transfer processes. The effect of period and amplitude variation on the temperature field of metals is the primary focus of this study.

A change in the temperature field is observed to have an effect on the temperature field's variation [19], [20]:

$$\Delta t_b(\tau) = \frac{T_{b,x+1}(\tau) - T_{b,x}(\tau)}{\Delta T_c}, \quad (10)$$

$$\Delta t_c(\tau) = \frac{T_{c,x+1}(\tau) - T_{c,x}(\tau)}{\Delta T_c} \quad (11)$$

Both Δ,b-b.(τ) and Ω,b-c.(τ) describe the surface temperature relative changes and the temperature differential at time τ, respectively. In units of $m^2K^2W^{-1}$, the amplitude change is quantified, whereas the periodic change is quantified in units of Ks^{-1}.$\cdot T$-b,x.(τ) and,T-b,x+1.(τ), where W is the surface temperature of the metal material before and after the characteristic parameter change. The difference in temperature (h) between the metal material's section after and before the parametric characteristics alteration is denoted as T-c,x.(τ) and T-c,x+1.(τ). The change induced by the boundary change is

denoted by Δ,T-c. The unit is K for changes in amplitude and b for changes in period.

A change in the boundary conditions causes a shift in the relative temperature, which in turn shows how the temperature field changes as the metal material moves in a certain direction. In order to understand the impact of varying temperatures and the same variation of these factors, the analysis of field temperature relies on constant change of distinguishing parameters.

In each iteration, the starting vibration amplitude is used to determine a 1% increase in amplitude. A twenty-fold run of surface temperature and break-to-break temperature differential calculations was done. The two of their outcomes to examine the change rule was selected.

The temperature and amplitude changes of the metal surface as a function of time during laminar cooling are shown in Fig 4. The variations in surface temperature of the metal material as it flows through each nozzle are depicted by the distribution curve, the form of which is dictated by the heat transfer coefficient. Equation 10 shows the relative change is negative when comparing the temperature surface after and before an increase in amplitude. As the surface temperature rises progressively along the metal substance's running direction due to the cumulative impact, it reaches its maximum value of -0.38 $m^2 \cdot K^2 W^{-1}$ in the tenth region. Δtb = -0.14 $m^2 \cdot K^2 W^{-1}$ is demonstrated in Fig 5 (b) during the 19th century, when amplitude grows from 1.03 to 1.05 times of initial amplitude. On the top, surface temperature relative change rises first in continuous change process at the same time as the amplitude steadily grows.

Nevertheless, relative change of surface temperature simultaneously falls as amplitude increases after 55.6 s. At 60 seconds, as illustrated in Fig 5 (b), $\Delta tb = -0.34 m^2 \cdot K^2 W^{-1}$ when the initial amplitude grows from 1.03 to 1.05 times, and $\Delta tb = -0.35 m^2 \cdot K^2 W^{-1}$ when the original amplitude rises from 1.1 to 1.13 times. The two main factors influencing the surface temperature of metals - the heat transfer coefficient and the temperature differential between the metals and the cooling water are responsible for this phenomenon. As the amplitude grows, the temperature differential between the metals and the water used for cooling becomes less. Consequently, the relative trend of decreasing changes in surface temperatures of metals is slowing down.

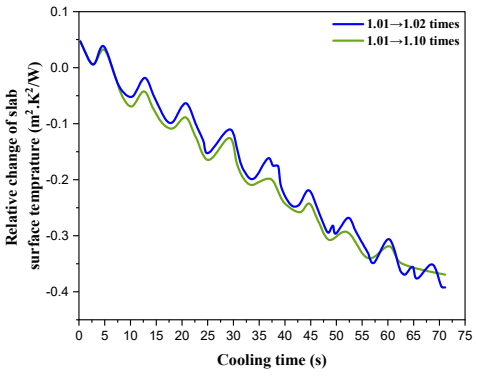

Figure 4. Relative temperature change of metal samples as sine amplitude raised

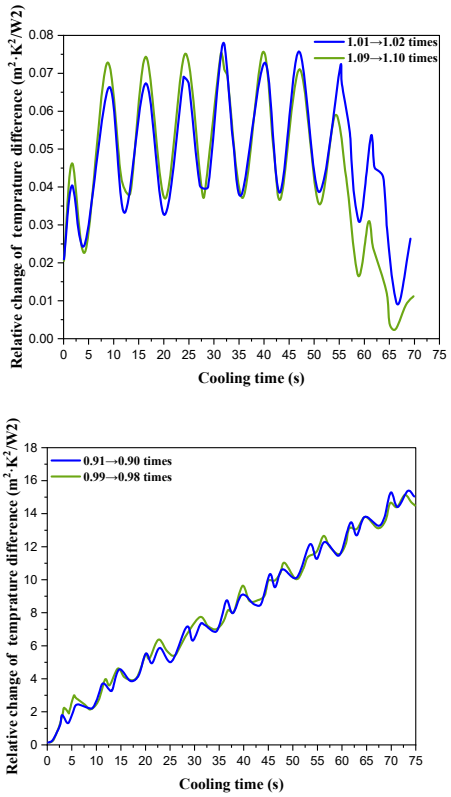

Figure 5. Temperature difference of metal samples relative to (a) an increase in sine amplitude (b) reduction in the sine amplitude

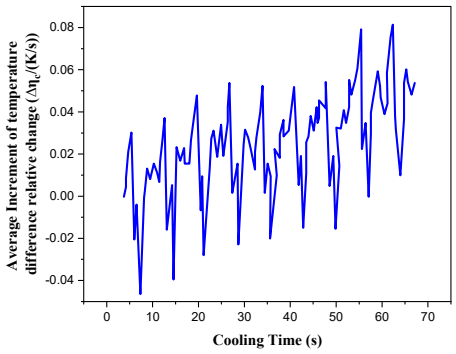

Figure 6. Surface temperature relative change on average as the interval gets shorter

Fig 6 shows the change in the relative temperature differential between the metal substance and the other material as the amplitude increases. There is an increase in cooling intensity, heat transfer coefficient, and amplitude in every injection location. Metals undergo rapid and noticeable changes to their surface temperatures, but their inside temperatures are impacted by their heat conduction performance and fluctuate at a much slower and smaller rate. Therefore, as metals move in a certain direction, a distribution curve of the temperature relative change differential among breaks may be seen. As the amplitude grows, Fig 5 (a) shows that relative variation of temperature difference is on rise. For example, in 22 seconds, when the amplitude goes from 1.03 times to 1.05 times, Δtc=0.038m2·K2W−1, and when it goes from 1.1 to 1.13 times, $\Delta tc = 0.045$ $m^2 \cdot K^2 W^{-1}$. The temperature difference on relative change after 45.1 s tends to decrease

with increasing amplitude, though. Fig 5 (a) shows that at 65 seconds, the Δtc increases from 0.033 $m^2 \cdot K^2 W^{-1}$ to 0.015 $m^2 \cdot K^2 W^{-1}$, while amplitude doubles from 1.1 times, starting amplitude to 1.15 times to original amplitude. The primary explanation for this occurrence is because the cooling range of metals increasingly expands as the amplitude increases. As time goes on, relative change increase of temperature difference among breaks gradually diminishes due to the cumulative effect. Typically, relative change in temperature is negligible, with a maximum value of 0.1 $m^2 \cdot K^2 W^{-1}$.

By starting with original cycle as a reference, we can lower it by 1% at each iteration (the initial modification being 0.1 times the original cycle), and we can keep going until we reach a reduction of 20%. Fig 5 (b) shows the results of two of these calculations that were used to analyse the change rule. Metal cooling rates drop and surface temperatures rise gradually as the period drops because the area covered by the sine function of the heat transfer coefficient (the area for water cooling) falls and the heat transfer coefficient falls simultaneously in half sine wave function dispersal. In last region, the relative surface temperature change attained a highest value of 14.12 K/s, as can be observed from Equation (10). Fig 5 (b) shows that a periodic drop area, denoted by the dotted circle, will form in neighboring region of any two adjacent regions when the relative surface temperature change is considered. This is mostly due to the fact that in this particular area, product of air-cooled area grows as cycle decreases, and the surface temperature of metals has the greatest impact on air-cooled area coefficient of heat transfer. When compared to water-cooled region, the difference is substantial. The Fig 6 shows that the change rate of Δηc can be observed from −0.06 to 0.09 K/s, and still noticeable features in every area. However, the increase value is quite less, suggesting that relative temperature change remains nearly constant as the period continuously decreases.

$$\Delta\eta_c = \frac{\Delta t_{c,N}(\tau) - \Delta t_{c,1}(\tau)}{N}, \tag{12}$$

where $\Delta,t\text{-}c,N.(\tau)$ represents the relative changes of temperature differential in material section at N^{th} time and $,t\text{-}c,1.(\tau)$ represents the same change at the first time, and N=22 represents the change in total time. Fig 7 shows that the relative change in temperature occurs as the period changes.

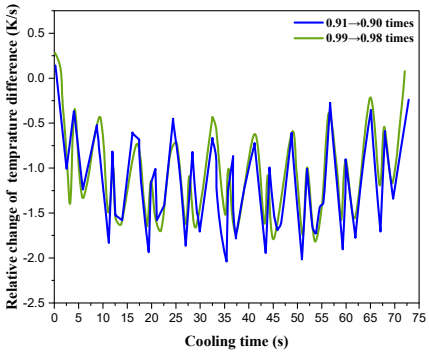

Figure 7. The temperature difference of metal samples as a function of decreasing sine period

Reducing the cycle, cooling intensity, and coefficient of heat transfer are goals in each injection zone. Although changes in the metal's surface temperature are readily apparent, its internal temperature was impacted by performance of heat conduction, which causes a delay in the change phase and a relatively small change quantity. There is a linear relationship between the decreasing cycle and the increasing air cooling interval between neighbouring injection locations. As a result, the metal material portion's relative change in temperature differential will show a peak value (node in Fig 7). The decline in cycle is correlated with the location of this peak value.

The mean increment of section temperature differential relative change at any given time when the period fluctuates continuously is defined by formula (13) [21], [22]:

$$\Delta\eta_c = \frac{\Delta t_{c,N}(\tau) - \Delta t_{c,1}(\tau)}{N} \tag{13}$$

where $\Delta,t\text{-}c,N.(\tau)$ represents the relative changes of temperature differential in material section at N^{th} time and $,t\text{-}c,1.(\tau)$ represents the same thing at the first time, and $N = 20$ is the change time. The mean increment dispersal of relative change of section temperature differential exhibits periodical behaviour when cycle decreases continuously, as shown in Fig 8, with a variation range of −0.08 to 0.08 K s^{-1}. The regions that experience significant fluctuations are located in close proximity to one another, and when the cycle decreases, the region undergoes a transition from air to water cooling. Looking at Fig 8, it is clear that the value of Δηc is quite modest. This means that while the period reduces continually, the change of relative temperature difference throughout section remains almost constant throughout.

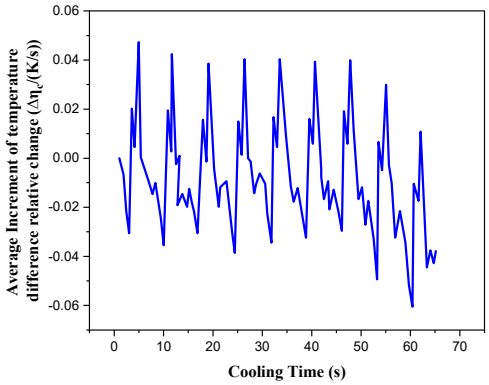

Figure 8. Temperature difference average increase relative shift when the duration shortens

5. CONCLUSION

This study proposes a method for obtaining parameter characteristic of metal materials' laminar cooling coefficients of heat transfer using field data, operational parameters, and structural parameters, and then analyses the effect of these parameters on the temperature field: Laminar cooling units' heat transfer boundary functions are piecewise functions that include a sine function and a straight line passing through middle of nozzle. Amplitude, period, and starting phase are the defining characteristics. A curve distribution of the surface temperature is observed, with a steady decline, as the amplitude increases and follows direction of movement of material. The surface temperature's relative change peaks in the last zone at −0.38 $m^2 \cdot K^2 W^{-1}$. The general trend is to rise initially before falling, with a maximum change value of 0.09 $m^2 \cdot K^2 W^{-1}$ and a curvilinear shift in relative change of the section temperature differential. As time declines, the surface temperature follows the direction of metal flow and

progressively increases, exhibiting a curve distribution. In last region, surface temperature relative change is at its peak at 14.56 K s^{-1}. The section temperature difference similarly follows a curve dispersal for its relative variation, reaching a highest value of about 2.8 K/s. However, this relative fluctuation is minor.

6. REFERENCES

[1] C.-N. Tong and Y.-D. Gao, "A useful method of building the heat transfer coefficient model in steel cooling process," *Kang T'ieh/Iron and Steel (Peking)*, 46, 7, 2011, pp. 50–55. DOI:10.13228/j.boyuan.issn0449-749X.2011465055

[2] M. Wang, *et al.,* "Experimental study on the laminar cooling process of the middle and heavy plate," in *Applied Mechanics and Materials*, 2012, pp. 808–811. DOI:10.4028/www.scientific.net/AMM.232.808

[3] A. Cebo-Rudnicka, *et al.,*"Inverse determination of the heat transfer coefficient distribution on a steel plate cooled by a water spray nozzle," in *WIT Transactions on Engineering Sciences*, 2012, pp. 345–355. DOI:10.2495/HT120301

[4] W.-L. Wu, *et al.,*"The study of improving the strip flatness in run-out-table during laminar cooling," *International Journal of Advanced Manufacturing Technology*, 95, 9–12, 2018, pp. 4419–4437. DOI:10.1007/s00170-017-1558-5

[5] Tian, Xiao-li., Zhang, Jie., Li, Hong-bo., Guo, Jie., "The effect of laminar cooling heat transfer coefficient on the temperature field of steel plate". Academic Search Premier, 2021-10, Vol.48 (9), p.1076-1082. DOI:10.1080/03019233.2021.1915646

[6] Yang, Jian ., WANG, J. L., LIU, W. H., "Modeling and Experimental Study of Inverse Heat Conduction Problems of Heavy Plate Laminar Cooling Process". International Conference on Computer Networks and Communication Technology, volume 54.DOI:10.2991/cnct-16.2017.56.

[7] YU W., LU, X. j., CHEN, Y. l., XU, Y. W., "Effect of coiling temperature on residual stresses in hot-rolled X70 pipeline steel strips during laminar cooling". Chinese Journal of Engineering, 2011, 33(6): 721-726. DOI: 10.13374/j.issn1001-053x.2011.06.014

[8] Y. Q. Zheng and J. Y. Cui, "FE analysis of hot strips' temperature distribution in laminar cooling process," in *Advanced Materials Research*, 2014, pp. 647–650. DOI:10.4028/www.scientific.net/AMR.900.647

[9] N. H. Bhatt, *et al.,*"High mass flux spray cooling with additives of low specific heat and surface tension: A novel process to enhance the heat removal rate," *Appl Therm Eng*, 120, 2017, pp. 537–548. DOI:10.1016/j.applthermaleng.2017.03.137

[10] W. Liu, *et al.,*"Experimental Study of Laminar Cooling Process on Temperature Field of the Heavy Plate," in *IOP Conference Series: Materials Science and Engineering*, 2018. DOI:10.1088/1757-899X/452/2/022034

[11] J. Pian, *et al.,*"Study of heat transfer parameters in the laminar cooling process for hot-rolled strips," in *Advanced Materials Research*, 2012, pp. 154–159. DOI:10.4028/www.scientific.net/AMR.546-547.154

[12] O. Resl and M. Pohanka, "The effect of remaining water layer on final temperature of steel plate during hot rolling," in *METAL 2019 - 28th International Conference on Metallurgy and Materials, Conference Proceedings*, 2019, pp. 355–360. DOI:10.37904/metal.2019.695

[13] Y. Song, *et al.,*"High-precision coiling temperature control model for heavy gauge strip steel," *Gongcheng Kexue Xuebao/Chinese Journal of Engineering*, 37, 1, 2015, pp. 106–110. DOI:10.13374/j.issn2095-9389.2015.01.016

[14] Angel Serrano, Ignacio Garrido, Elena Palomo Del Barrio, Manuel Carmona,"Effect of processing on microstructure and mechanical properties of pentaglycerine based solid-solid phase change materials". Journal of Energy Storage, Vol 55,2022, 105677. DOI: 10.1016/j.est.2022.105677

[15] L.-Y. Jiang, *et al.,*"Analysis of heat transfer coefficients during high intensity cooling processes of hot rolled strips after rolling," *Dongbei Daxue Xuebao/Journal of Northeastern University*, 35, 5, 2014, pp. 676–680. DOI:10.12068/j.issn.1005-3026.2014.05.016

[16] U. Muhin, S. Belskij, E.Makarov, T. Koynov,"Simulation of accelerated strip cooling on the hot rolling mill run-out roller table
". U. Muhin et alii, Frattura ed Integrità Strutturale, 37 (2016) 305-311 DOI: 10.3221/IGF-ESIS.37.40

[17] H.-M. Wang, *et al.,*"Effect of water flow rate on the heat transfer coefficient of a hot steel plate during laminar flow cooling," *Beijing Keji Daxue Xuebao/Journal of University of Science and Technology Beijing*, 34, 2012, 12, pp. 1421–1425. DOI:10.13374/j.issn1001-053x.2012.12.008shu

[18] S. Zhang, *et al.,*"Research on Mathematical Model of Inverse Heat Conduction Problem in Laminar Cooling Process," in *Proceedings of 2018 IEEE 3rd International Conference on Cloud Computing and Internet of Things, CCIOT*, 2018, pp. 444–447. DOI:10.1109/CCIOT45285.2018.9032459

[19] B.-L. Deng and X.-R. Zhang, "Flow stability of laminar supercritical CO2 sudden expansion flow with field synergy principle," in *2010 14th International Heat Transfer Conference, IHTC, 14*,2010, pp. 533–538. DOI:10.1115/IHTC14-22464

[20] Z. Malinowski, *et al.,*"Implementation of the axially symmetrical and three dimensional finite element models to the determination of the heat transfer coefficient distribution on the hot plate surface cooled by the water spray nozzle," in *Key Engineering Materials*, 2012, pp. 1055–1060. DOI:10.4028/www.scientific.net/KEM.504-506.1055

[21] J. Wang, *et al.,*"Research on solve of heat transfer coefficients and experimental of the heavy plate in laminar cooling process," in *Journal of Physics: Conference Series*, 2020. DOI:10.1088/1742-6596/1650/2/022115

[22] S. Li, *et al.,*"A T-S fuzzy model-based intelligent temperature prediction model of laminar cooling system," in *Proceedings - 2015 Chinese Automation Congress, CAC, 2015*, 2016, pp. 1221–1224. DOI:10.1109/CAC.2015.7382685v